

Development of a multiaxial deformation measure and creep-fatigue damage summation for multiple load cycle types in support of an improved creep-fatigue design method

Applied Materials Division

About Argonne National Laboratory

Argonne is a U.S. Department of Energy laboratory managed by UChicago Argonne, LLC under contract DE-AC02-06CH11357. The Laboratory's main facility is outside Chicago, at 9700 South Cass Avenue, Argonne, Illinois 60439. For information about Argonne and its pioneering science and technology programs, see www.anl.gov.

DOCUMENT AVAILABILITY

Online Access: U.S. Department of Energy (DOE) reports produced after 1991 and a growing number of pre-1991 documents are available free at OSTI.GOV (<http://www.osti.gov/>), a service of the U.S. Dept. of Energy's Office of Scientific and Technical Information

Reports not in digital format may be purchased by the public from the National Technical Information Service (NTIS):

U.S. Department of Commerce
National Technical Information Service
5301 Shawnee Rd
Alexandria, VA 22312
www.ntis.gov
Phone: (800) 553-NTIS (6847) or (703) 605-6000
Fax: (703) 605-6900
Email: **orders@ntis.gov**

Reports not in digital format are available to DOE and DOE contractors from the Office of Scientific and Technical Information (OSTI)

U.S. Department of Energy
Office of Scientific and Technical Information
P.O. Box 62
Oak Ridge, TN 37831-0062
www.osti.gov
Phone: (865) 576-8401
Fax: (865) 576-5728
Email: **reports@osti.gov**

Disclaimer

This report was prepared as an account of work sponsored by an agency of the United States Government. Neither the United States Government nor any agency thereof, nor UChicago Argonne, LLC, nor any of their employees or officers, makes any warranty, express or implied, or assumes any legal liability or responsibility for the accuracy, completeness, or usefulness of any information, apparatus, product, or process disclosed, or represents that its use would not infringe privately owned rights. Reference herein to any specific commercial product, process, or service by trade name, trademark, manufacturer, or otherwise, does not necessarily constitute or imply its endorsement, recommendation, or favoring by the United States Government or any agency thereof. The views and opinions of document authors expressed herein do not necessarily state or reflect those of the United States Government or any agency thereof, Argonne National Laboratory, or UChicago Argonne, LLC.

Development of a multiaxial deformation measure and creep-fatigue damage summation for multiple load cycle types in support of an improved creep-fatigue design method

Applied Materials Division
Argonne National Laboratory

June 2019

Prepared by

M. C. Messner, Argonne National Laboratory
T.-L. Sham, Argonne National Laboratory

Abstract

This report describes methods for extending the elastic perfectly plastic (EPP) simplified model test (SMT) approach to cover multiaxial load conditions and methods to combine EPP+SMT use fractions for multiple loading cycles. The completion of this work, in conjunction with companion reports on constructing and validating SMT design curves, marks the development of a complete methodology for assessing creep-fatigue damage in high temperature nuclear reactor structural components. This EPP+SMT method aims to better account for elastic follow up effects, simplify the design process, and reduce overconservatism when compared to current simplified bounding approaches in the ASME Boiler and Pressure Vessel Code Section III, Division 5, Subsection HB, Subpart B covering high temperature nuclear reactors.

Table of Contents

Abstract	i
Table of Contents	iii
List of Figures	v
List of Tables	vii
1 Introduction	1
2 Multiaxiality	3
2.1 Objective	3
2.2 The Huddleston model	3
3 Multiple load cases	9
3.1 Motivation	9
3.2 Recommended procedure	9
3.2.1 Method	9
3.2.2 Load cycle combination procedures	11
3.2.3 Comparison between methods	14
3.2.4 Comparison to design by inelastic analysis	16
3.3 Recommended approach: modified composite cycles	16
4 Conclusions	21
Acknowledgments	23
Bibliography	25

List of Figures

3.1	SMT design chart constructed to be consistent with the inelastic model and the ASME method of design by inelastic analysis. In order from longest life to shortest life the diagram shows lines for no hold (the ASME unfactored fatigue diagram), 1 hour, 10 hour, 100 hour, 1,000 hour, and 10,000 hour holds.	11
3.2	Diagram illustrating Option A. The half cycle strain ranges are the true peak-to-valley or valley-to-peak strain ranges in a full transient analysis of the complete load history.	12
3.3	Diagram illustrating Option B. (a) Conceptual framework of block loading. (b) Actual method for computing strain ranges and hold times.	13
3.4	Diagram illustrating option C. Load cycles are analyzed individually and then superimposed using some assumed order.	13
3.5	Diagram illustrating Option E, the composite cycle approach currently used in other ASME design methods using elastic perfectly-plastic analysis.	14
3.6	Bar chart comparing the number of times the predicted cyclic life fraction from Options B, C, and D exceeds or fails to exceed the life fraction predicted by Option A.	15
3.7	Histogram comparing the life ratio between each of Options B, C, and D and Option A. Cases to the right of the dashed line are conservative.	15
3.8	Comparison between the ASME Section III, Division 5 design by inelastic analysis method for creep-fatigue evaluation and the EPP+SMT method with consistent design charts. Subfigures a, b, c, d, and e plot data for Options A, B, C, D, and E, respectively. The points are located at the fatigue and creep damage calculated with the design by inelastic analysis method. The black line shows the interaction diagram. The colors indicate the EPP+SMT results: blue means the load combinations pass the EPP+SMT method, red means they fail. Note none of the conditions examined here pass the current EPP+SMT criteria (see text for additional details).	17
3.9	Illustration of the proposed composite cycle approach. (a) Load histogram. (b) Composite cycles developed from the load histogram. Regions assigned to each Service Load, weights, and the composite cycle periods are indicated on the plot. Load conditions marked with a * are fictitious connector segments. (c) Notional analysis results from a shakedown analysis of each composite load cycle. The effective strain range and individual service load time are indicated on the figure.	20

List of Tables

2.1	Huddleston constants for the Class A materials drawn from the ASME Code.	4
3.1	Parameters used to generate 200 random strain cycle histories.	14

1 Introduction

This report extends a new method for creep-fatigue design of high temperature nuclear reactor structural components to account for multiaxial loading and multiple load cycle combinations. The new method is called the EPP+SMT approach because it uses an elastic perfectly-plastic (EPP) analysis in conjunction with design curves accounting for elastic follow up calibrated to simplified model test (SMT) data. The overall goals of the new approach are to:

1. Better account for elastic follow up in high temperature creep-fatigue design.
2. Simplify the process of completing the design of a component.
3. Reduce overconservatism, where possible, compared to current creep-fatigue design methods in the ASME Boiler and Pressure Vessel Code Section III, Division 5, Subsection HB, Subpart B [1].

This report focuses on two limited aspects of the new method. The origins of the overall EPP+SMT approach are in past work on accounting for elastic follow up in creep-fatigue design and analysis [2]. Past DOE sponsored research has completed the development of the SMT test specimen, designed to directly assess the effect of follow up on high temperature cyclic life [3, 4, 5, 6, 7]. Additional past work developed the EPP analysis method used to estimate strain ranges in the new design approach [8]. Finally, companion reports to be published in 2019 develop SMT design curves from experimental creep-fatigue and SMT data and simplify the process of running SMT tests by developing a test method that uses a standard creep-fatigue test specimen and a single load frame.

Taken in its totality, this past and companion work completes a EPP+SMT design method can be applied to uniaxial structures subject to a single periodic load cycle. Actual reactor components will experience multiaxial deformation and the combination of many different transient loads. This report extends the EPP+SMT method to account for these effect. The result is a complete design method on par with current ASME and international approaches [9, 10, 11] that can be used to generate designs for high temperature reactor structural components.

Chapter 2 of this report describes the extension of the uniaxial method to multiaxial loading by defining an appropriate effective strain measure accounting for multiaxial effects on creep and fatigue damage and deformation. Chapter 3 then extends the approach to handle multiple load cases, in the end recommending a modified composite load cycle approach of the type current used in other ASME EPP design methods [12, 13]. Finally, Chapter 4 summarizes the recommendations made here and describes the future work required to validate the complete EPP+SMT design method and codify it through an ASME nuclear Code Case.

2 Multiaxiality

2.1 Objective

The base EPP+SMT method has been formulated using uniaxial test data. Extensive past research establishes that the multiaxial stress field strongly influences creep rupture life [14, 15] and that this multiaxiality effect depends on the particular material [16, 17]. The final EPP+SMT design method must therefore account for the effect of stress multiaxiality on creep-fatigue cyclic life. Even in simple vessel structures the stresses are biaxial and realistic components have substantial triaxial stresses near structural discontinuities like nozzles. The traditional method for handling stress triaxiality is to develop a scalar effective stress measure, a map from a general state of stress to a scalar, that correlates the available multiaxial rupture data to the uniaxial data. This general approach is adopted here but, as the EPP+SMT approach uses strain ranges instead of stresses, this section defines a scalar effective strain range that incorporates the effect of multiaxiality.

Ideally, this effective strain measure would be created by synthesizing the results of multiaxial SMT tests. To be comprehensive, such a testing methodology would need to incorporate independently controlled multiaxial strain ranges with elastic follow up. Traditional multiaxial creep effective stresses correlate rupture time to the material stress state. Previous work uses pressurized tubes, pressurized tubes under axial stresses [18], or stress-controlled tension-torsion tests [19, 20, 21]. The pressurized tests are not suitable for the strain-based SMT approach, but tension-torsion tests could be used to generate biaxial SMT data to support the development of an effective strain measure. The ideal test would generalize the one-bar SMT specimen concept, described in a companion report from Oak Ridge National Laboratory (ORNL), that uses a standard specimen in combination with electronic controls to apply load through elastic-follow up without needing specialized test geometries. The tension-torsion equivalent of this test could impose independently controlled axial and torsional strain and follow up factors. This test would generate biaxial strain states. The final effective strain measure could be validated against triaxial strain configurations. There are no common, well-validated test specimens for controlling general triaxial loading, whether stress or strain controlled. However, notched specimens with various notch geometries can be used to examine the effect of triaxial loading in conjunction with numerical modeling to determine the strain field [22, 23, 24].

In the absence of these specialized tests this section uses an existing validated model for the effect of stress triaxiality on rupture life to define a suitable EPP+SMT effective strain measure. This solution avoids the development of specialized multiaxial SMT specimens. However, the effective strain measure defined here should be validated in the future with multiaxial creep-fatigue test data.

2.2 The Huddleston model

The current version of Section III, Division 5, Subsection HB, Subpart B, Nonmandatory Appendix HBB-T [1] uses the Huddleston stress [18] to convert multiaxial stress states to a uniaxial effective stress used to calculate creep damage when using the design by inelastic analysis approach. The Huddleston model was calibrated to uniaxial and biaxial creep test data gathered from a variety of sources in the form of standard creep tests, pressurized tube

Material	C
304H	0.24
316H	0.24
800H	0
2.25Cr-1Mo	$\begin{cases} 0.16 & I_1/I_S \geq 1 \\ 0 & I_1/I_S < 1 \end{cases}$
Grade 91	$\begin{cases} 0.16 & I_1/I_S \geq 1 \\ 0 & I_1/I_S < 1 \end{cases}$
Alloy 617	0.24

Table 2.1: Huddleston constants for the Class A materials drawn from the ASME Code.

tests, pressurize + tension tests, and tension-torsion tests. The data was correlated to develop the model and corresponding parameters for the current Class A materials. The form of the effective stress is

$$\sigma_h = \sigma_v \exp \left[C \left(\frac{I_1}{I_S} - 1 \right) \right] \quad (2.1)$$

with σ_v the von Mises effective stress

$$\sigma_v = \sqrt{\frac{(\sigma_1 - \sigma_2)^2 + (\sigma_2 - \sigma_3)^2 + (\sigma_3 - \sigma_1)^2}{2}}, \quad (2.2)$$

I_1 is the first invariant of the stress

$$I_1 = \sigma_1 + \sigma_2 + \sigma_3, \quad (2.3)$$

I_S is an additional invariant

$$I_S = \sqrt{\sigma_1^2 + \sigma_2^2 + \sigma_3^2}, \quad (2.4)$$

and C is a parameter, fit to the biaxial test data. Table 2.1 reproduces the values of C found in the the in-progress nuclear Code Case making Alloy 617 a Class A material and Section III, Division 5 (for the remaining materials). Note that for $C = 0$ or for uniaxial load ($\sigma_2 = \sigma_3 = 0$) the Huddleston stress degenerates to the von Mises stress.

For fatigue and for design by inelastic analysis, Section III, Division 5 uses the effective strain range

$$\Delta \varepsilon_e = \frac{\sqrt{2}}{3} \sqrt{(\Delta \varepsilon_x - \Delta \varepsilon_y)^2 + (\Delta \varepsilon_y - \Delta \varepsilon_z)^2 + (\Delta \varepsilon_z - \Delta \varepsilon_x)^2 + \frac{3}{2} (\Delta \gamma_{xy}^2 + \Delta \gamma_{yz}^2 + \Delta \gamma_{zx}^2)} \quad (2.5)$$

which is the so-called ‘‘von Mises strain’’ *if the material is incompressible*, except instead of the absolute strain tensor this definition of an equivalent strain range uses the difference in the strain tensors between two points in time.

The von Mises stress and the increment of the von Mises strain are related by being work conjugate. The von Mises stress and strain increment are, in terms of the deviatoric stress \mathbf{s} and deviatoric plastic strain \mathbf{e}_p

$$\sigma_v = \sqrt{\frac{3}{2} \mathbf{s} : \mathbf{s}} \quad (2.6)$$

and

$$d\varepsilon_v = \sqrt{\frac{2}{3} d\mathbf{e}_p : d\mathbf{e}_p}. \quad (2.7)$$

The total inelastic work increment is

$$dW = \boldsymbol{\sigma} : d\boldsymbol{\varepsilon}_p = \mathbf{s} : d\mathbf{e}_p + \mathbf{p} : d\mathbf{h}_p \quad (2.8)$$

where \mathbf{p} is the hydrostatic stress and \mathbf{h} is the hydrostatic inelastic strain. Provided plastic deformation is incompressible the work increment degenerates to

$$dW = \mathbf{s} : d\mathbf{e}_p. \quad (2.9)$$

For common theories of plasticity the deviatoric stress and the inelastic strain are colinear – that is

$$\mathbf{s} = k d\mathbf{e}_p \quad (2.10)$$

for some scalar k . Then note

$$\sigma_v d\varepsilon_v = \sqrt{\frac{3}{2} \mathbf{s} : \mathbf{s}} \sqrt{\frac{2}{3} d\mathbf{e}_p : d\mathbf{e}_p} = \sqrt{\frac{3}{2} k d\mathbf{e}_p : k d\mathbf{e}_p} \sqrt{\frac{2}{3} d\mathbf{e}_p : d\mathbf{e}_p} = k d\mathbf{e}_p : d\mathbf{e}_p = \mathbf{s} : d\mathbf{e}_p = dW \quad (2.11)$$

thus proving the von Mises stress and von Mises strain increment are work conjugate for incompressible materials where the inelastic strain is colinear with the deviatoric stress.

The concept of work conjugate stress and strain measures is key in that in standard plasticity theory a flow surface defined by a scalar effective stress will lead to a increment in plastic strain with a magnitude defined by the work conjugate effective strain [25]. So the conjugate strain to some stress measure used to define inelastic flow is the natural equivalent of that stress measure in strain space. For $C = 0$ the ASME Code applies this concept in the definition of effective stress, used to compute damage induced by inelastic creep deformation, and the effective strain used to compute fatigue damage.

The EPP+SMT does not separate out creep and fatigue damage, instead basing the life calculation only on a strain measure. For uniaxial loading the design data has been calibrated to the axial strain. This places one constraint on the choice of an effective strain measure – it should degenerate to the axial strain for uniaxial deformation. By convention, the Code treats analysis results from inelastic methods, including EPP methods, as fully-incompressible, neglecting the small compressible elastic strain. So it will be sufficient that the effective strain measure degenerates to the axial strain for incompressible uniaxial deformation.

The standard effective strain used to calculate fatigue damage in the Code (Eq. 2.5) is a viable option. It degenerates to the axial strain for incompressible uniaxial deformation and is conjugate to the stress measure used to define the flow surface for J_2 plasticity and creep theories. For materials where creep damage follows a J_2 -type relation it would be a perfectly

reasonable strain measure to selected for the EPP+SMT theory. However, the ASME Code in the form of the Huddleston stress already asserts that creep damage in some of the Class A materials does not follow a standard J_2 theory. As creep damage in the Code is one component of creep-fatigue damage, it would be reasonable then to use the strain measure conjugate to the Huddleston stress to account for creep-fatigue damage for these materials.

Calculating this strain is, at least conceptually, straightforward

$$dW = \boldsymbol{\sigma} : d\boldsymbol{\varepsilon}_p = \sigma_h d\varepsilon_h \quad (2.12)$$

$$d\varepsilon_h = \frac{\boldsymbol{\sigma} : d\boldsymbol{\varepsilon}_p}{\sigma_h}. \quad (2.13)$$

It will be convenient to consider the volumetric and deviatoric parts separately:

$$d\varepsilon_h = \frac{\mathbf{s} : d\mathbf{e}_p + \mathbf{p} : d\mathbf{h}_p}{\sigma_h} = \frac{\sigma_v d\varepsilon_v + \mathbf{p} : d\mathbf{h}_p}{\sigma_v \exp \left[C \left(\frac{I_1}{I_S} - 1 \right) \right]}. \quad (2.14)$$

Then for incompressible plasticity

$$d\varepsilon_h = \frac{\mathbf{s} : d\mathbf{e}_p + \mathbf{p} : d\mathbf{h}_p}{\sigma_h} = \frac{\sigma_v d\varepsilon_v}{\sigma_v \exp \left[C \left(\frac{I_1}{I_S} - 1 \right) \right]} = \frac{d\varepsilon_v}{\exp \left[C \left(\frac{I_1}{I_S} - 1 \right) \right]}. \quad (2.15)$$

Define

$$F = \exp \left[C \left(\frac{I_1}{I_S} - 1 \right) \right] \quad (2.16)$$

then

$$d\varepsilon_h = \frac{d\varepsilon_v}{F}. \quad (2.17)$$

The problem with this expression is that the factor F refers to the material's stress state, not the strain tensor.

An alternate definition of F in terms of standard stress invariants is [26]

$$F = \exp \left[C \left(\frac{I_1}{\sqrt{\frac{6J_2 + I_1^2}{3}}} - 1 \right) \right] \quad (2.18)$$

where J_2 is the second invariant of the stress deviator.

For isotropic elastic deformation there is a relation between the first invariants of the stress and strain tensors

$$I_1 = \frac{K}{3} E_1. \quad (2.19)$$

The second deviatoric invariant relates to the von Mises stress:

$$\sigma_v^2 = 3J_2. \quad (2.20)$$

Combining these expressions

$$F = \exp \left[C \left(\frac{\frac{K}{3} E_1}{\sqrt{\frac{2\sigma_v^2}{3} + \frac{K^2 E_1^2}{27}}} - 1 \right) \right]. \quad (2.21)$$

Which still involves the stress tensor. The mixed measure is unsatisfying as it requires both the stress and strain history of the component to calculate.

The final form of the proposed effective strain range measure is then

$$\Delta\varepsilon_{SMT} = \frac{\Delta\varepsilon_e}{F_{min}} \quad (2.22)$$

where $\Delta\varepsilon_e$ is the current ASME Code effective strain range, given in Eq. 2.5, F_{min} denotes the minimum value of F over the load cycle, and Eq. 2.16 defines the Huddleston factor. The expression should be used in conjunction with Table 2.1 giving the Huddleston coefficients for the Class A materials.

The odd part of this expression is that the effective strain is divided by the Huddleston factor F . This makes sense from a work conjugacy perspective as the triaxiality factors cancel when multiplied to produce the work increment. However, it is an odd result in that to find the maximum strain range the designer must find the minimum Huddleston factor.

An alternative definition of the EPP+SMT strain range might be

$$\Delta\varepsilon_{SMT} = F_{max}\Delta\varepsilon_e \quad (2.23)$$

$$F_{max} \geq 1 \quad (2.24)$$

where F_{max} is now the maximum Huddleston factor over the cycle. Constraining the maximum factor to be greater than 1 prevents the effective strain measure from being less than the standard von Mises strain measure used to correlate to fatigue damage in the current Code. This expression produces the expected result that increasing the Huddleston factor increases the cyclic damage. While less rigorous than the work-conjugate strain, the practical advantages of this strain measure outweigh this drawback.

A final option might simply to retain the standard ASME definition of effective strain until multiaxial SMT tests prove it to be inadequate. With this method, the EPP+SMT approach would degenerate to the current ASME approach to high temperature fatigue design for zero hold time. In the absence of better options we suggest retaining the current definite of effective strain range. We recommend the development of a multiaxial creep-fatigue test, similar to the single bar SMT test, that could be used to validate and compare alternate effective strain measures.

3 Multiple load cases

3.1 Motivation

Combining the previous chapter with the companion report on the EPP+SMT design method for uniaxial loading, the approach can now be applied to a realistic structure sustaining general stress states. However, the creep-fatigue and SMT test data used to calibrate the design curves only consider a single type of periodic loading. Actual components will be designed against multiple types of loading, conventionally expressed for design using the ASME Section III, Division 5 [1] methods as a collection of service loading conditions. At a minimum, the Design Specification must define each service loading and provide a histogram giving the number of repetitions for each individual load case. The Specification may also provide an anticipated loading order. A complete design method must provide a way to combine the effects of multiple design loadings into a single estimate of the component's cyclic creep-fatigue life.

Current ASME design methods use three different strategies to combine load cycles, depending on the design analysis method:

1. Design by elastic analysis: analyze each load case separately and superimpose the results.
2. Design by elastic perfectly-plastic analysis: use a bounding composite cycle that samples a single repetition of each service load.
3. Design by inelastic analysis: a full transient analysis of the component's service life, explicitly analyzing each repetition of each service load in order.

The method selected for use with the EPP+SMT design method should reflect the elastic perfectly-plastic analysis approach. For example, while superimposing loads would be ideal for design simplicity, the superposition principle does not apply to nonlinear EPP analysis.

3.2 Recommended procedure

3.2.1 Method

The approach used here to develop a method for combining load cycles is to test prospective methods using randomly generated loads. For the purpose of testing methods for combining load cases it is sufficient to consider uniaxial loading. The basic approach used to generate random loadings is:

1. For each of M different types of loads:
 - (a) Select a random maximum strain $\varepsilon_i \in [\varepsilon_{min}, \varepsilon_{max}]$
 - (b) Select a random hold time at maximum strain $t_i \in [0, t_{max}]$
 - (c) Select a random follow up factor for the hold $q_i \in [1, q_{max}]$
 - (d) Select a random loading strain range $\dot{\varepsilon}_i \in [\dot{\varepsilon}_{min}, \dot{\varepsilon}_{max}]$
 - (e) Select a random number of repetitions $N_i \in [1, N_{max}]$

2. Determine the transient uniaxial history by starting at $\varepsilon = 0$. Randomly select a repetition of a load cycle described by $(\varepsilon_i, t_i, q_i, \dot{\varepsilon}_i)$ from the remaining library of loads:
 - (a) Connect the current strain ε to the target strain ε_i by loading the bar at a strain rate of $\dot{\varepsilon}_i$
 - (b) Hold the structure at this strain for t_i , relaxing through a follow up factor of q_i .
3. Repeat this process until all repetitions N_i for all load cases M are exhausted.

The resulting strain history, as a function of time, can be used in conjunction with an inelastic constitutive model to determine the stresses as a function of time. The final time, strain, stress history can be used to calculate separate creep and fatigue damage fractions, according to the ASME design by inelastic analysis provisions. The relevant creep-fatigue interaction diagram can then be consulted as an acceptance criteria. In doing this analysis, the design factor of 0.67 on the stress relaxation history and the fatigue diagram factors of 2 on strain range and 20 on cycles to failure have been removed from the ASME procedure. The result of this process is a pass/fail. A more granular measure of adequacy can be developed by calculating the shortest distance between the calculated creep and fatigue damage plotted on the D-diagram and the design interaction creep-fatigue envelop.

The results of this inelastic analysis can be compared to a prospective EPP+SMT procedure. The analysis method and the basic acceptability test for uniaxial loading and a single load cycle have been developed in past reports [8]. The EPP analysis uses a pseudoyield stress determined by S_y and the value of the material's isochronous stress-strain curve at the current metal temperature, 0.2% inelastic strain (i.e. creep + plastic strain), and a time equal to the load cycle period. The acceptance test is a modified fatigue curve accounting for both hold time and elastic follow up, calibrated to both standard creep-fatigue and specialized SMT tests.

To test the adequacy of a load cycling combination procedure for the EPP+SMT method we consider inelastic analysis for 316H stainless steel using the Code design properties and an inelastic constitutive model developed at Argonne National Laboratory [27]. For the EPP+SMT method we use consistent design data. Because the loads are strain-controlled there is no need to run the EPP shakedown analysis and so consistent values of yield stress and consistent isochronous curves are not required. The SMT design charts are generated by starting with the unfactored ASME fatigue curve, running a simulation with the inelastic model for each strain range along the curve with a tensile hold for the time in question. The resulting time, strain, stress history can be used to calculate fatigue and creep damage, and the cycle repeated until the unfactored design by inelastic analysis method predicts cyclic failure. This number of cycles is used as the EPP+SMT design chart value for the given strain range and hold time, the process repeated to build up the design chart. The resulting EPP+SMT design information is consistent with the inelastic constitutive model. The objective in generating this consistent information is to test only the load cycle combination strategy and not the design data or the design method as a whole. For this exercise, all the loading is done at a constant temperature of 700° C and a follow up factor of $q = 1$. The random hold times are limited to 10,000 hours. Figure 3.1 plots the consistent SMT design chart used in this study.

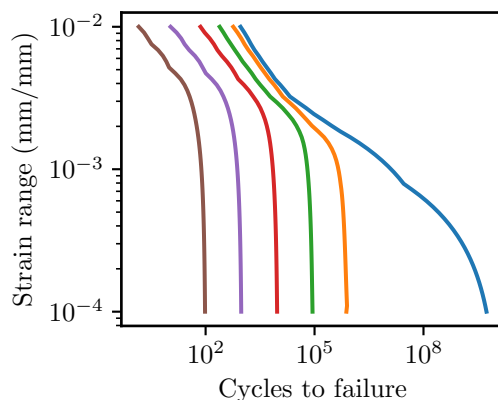


Figure 3.1: SMT design chart constructed to be consistent with the inelastic model and the ASME method of design by inelastic analysis. In order from longest life to shortest life the diagram shows lines for no hold (the ASME unfactored fatigue diagram), 1 hour, 10 hour, 100 hour, 1,000 hour, and 10,000 hour holds.

As with the inelastic analysis, the corresponding EPP+SMT analysis uses unfactored design data. The EPP+SMT method uses the usage fraction

$$D = \sum_{i=1}^n \frac{N_i}{N_{f,i}} \quad (3.1)$$

where N_i are the number of cycles for load type i and $N_{f,i}$ are the design allowable cycles for that same loading.

3.2.2 Load cycle combination procedures

Previous EPP methods use a composite load cycle approach for combining different load cases into a single EPP analysis. This approach combines the loading conditions from each of the individual load cases into a single, composite load cycle. The analysis then repeats this composite cycle in a shakedown analysis and uses the results in the acceptance procedure. The current EPP Code Cases do not provide guidance on the specifics of constructing this composite cycle, for example guidance on how the cycle order will affect the results of the design process. A composite cycle approach, instead of individual cycle analysis, was adopted because elastic perfectly-plastic analyses cannot be superimposed and requiring a full analysis of the component's load history would greatly complicate the design method. That said, because the random sample load histories used here are uniaxial and strain controlled, a full transient analysis is possible with the EPP+SMT method. The half-cycle strain range used is peak-to-valley range and the time used to enter the design charts is simply the total time between valley and peak or peak and valley (see Figure 3.2). This method is labeled Option A. For this option the sum of the cycle time times the number of half cycles will total to the design life. For general loading this method is not practical, but it can be used to assess other prospect approaches.

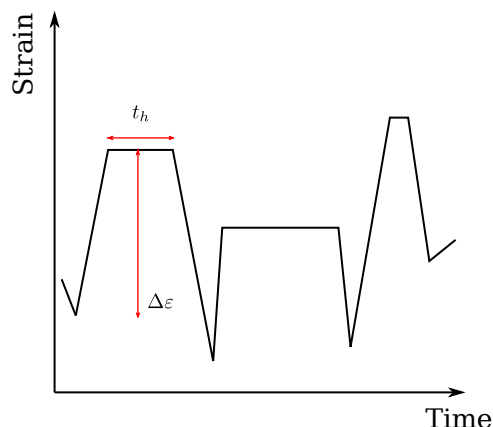


Figure 3.2: Diagram illustrating Option A. The half cycle strain ranges are the true peak-to-valley or valley-to-peak strain ranges in a full transient analysis of the complete load history.

In general, the principle of superposition cannot be used to combine or rearranged individual EPP cycle analysis. However, if the actual loading is done blockwise (Figure 3.3), where each load cycle is repeated the full N_i times before moving to the next type of load, the prior history in the EPP analysis essentially only sets the initial residual stress for the new block of loading. Cyclic plasticity (and elevated temperature creep) will quickly erase this past residual stress pattern and so the prior load history can be safely discarded. For block loading then each load cycle could be analyzed with a separate EPP calculation and the resulting damages combined using Eq. 3.1. Of course in actuality the loads on a reactor will not be applied in a block fashion, but nevertheless we include this method as Option B in the analysis below. Note this option attributes one full cycle from zero strain to the cycle strain and back for each repetition of a particular load. For this option the sum of the cycle time times the number of full cycles will total to the design life.

Option C (Fig. 3.4) is a variant of the previous approach. Here each cycle is analyzed individually and the effective strain range calculated. The cycles are then arranged in some order – here each repetition of each load cycle is uniformly distributed throughout the design life, but the order could also be given in the design specification. Assumed half cycles are then constructed by *summing* the effective strain range for adjacent pairs of cycles and associating the summed strain range with the hold time of first of the two loads. For the strain range this is a bounding assumption – maximum compressive strain to maximum tensile strain – and the half cycle lives will sum to the design life.

Option D is a simple variant of Option C. The method is exactly the same except that each peak to peak strain is attributed as a one full cycle.

Option E (Fig. 3.5) is the composite cycle approach. Here the designer would select a particular composite cycle order including one repetition of each cycle type and then calculate hold times and strain ranges from a shakedown analysis of this composite cycle. The use fraction for a single repetition of the load case could be calculated from this analysis, and then multiplied by the number of repetitions of that particular loading provided in the Design

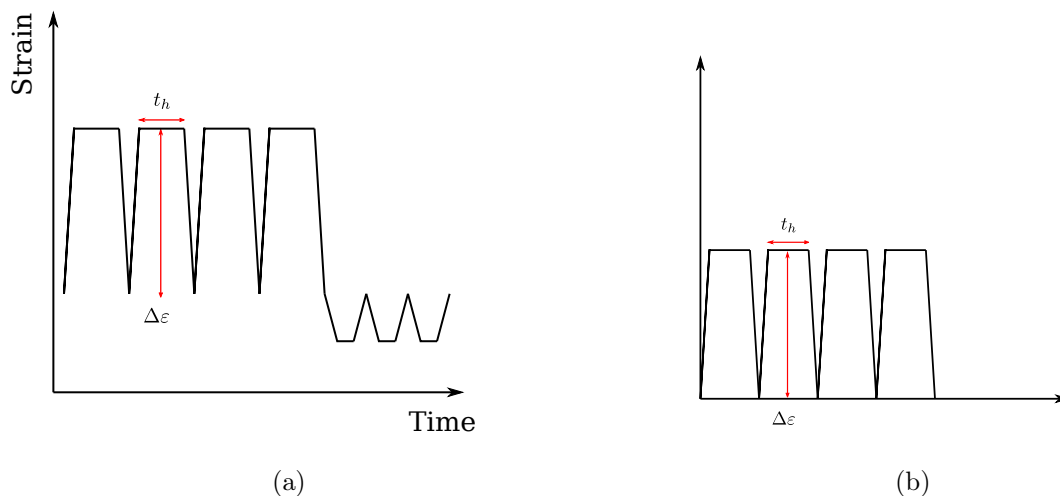


Figure 3.3: Diagram illustrating Option B. (a) Conceptual framework of block loading. (b) Actual method for computing strain ranges and hold times.

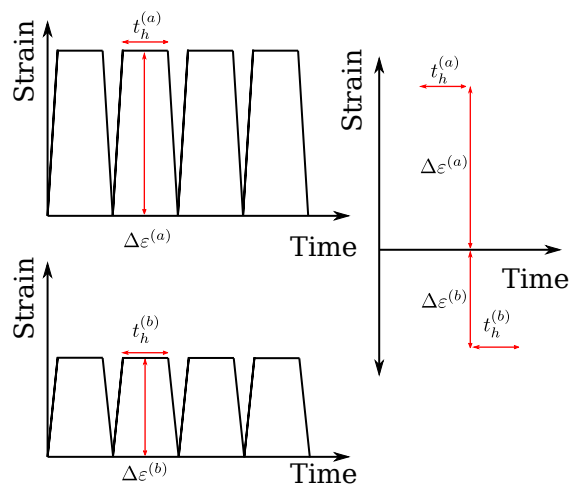


Figure 3.4: Diagram illustrating option C. Load cycles are analyzed individually and then superimposed using some assumed order.

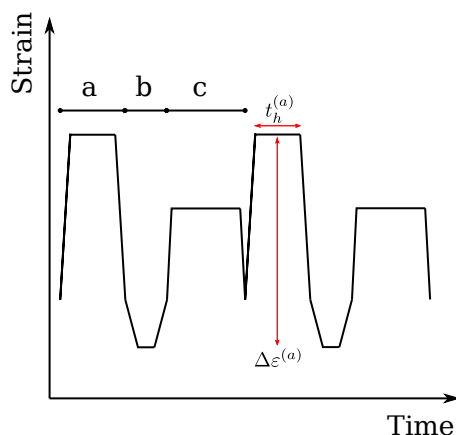


Figure 3.5: Diagram illustrating Option E, the composite cycle approach currently used in other ASME design methods using elastic perfectly-plastic analysis.

Parameter	Range or value
M	5
ε_i	$[-0.01, 0.01]$ mm/mm
t_i	$[0, 5000]$ hours
q_i	1.0
$\dot{\varepsilon}_i$	1.0 mm/mm/hr
N_i	$[1, 25]$

Table 3.1: Parameters used to generate 200 random strain cycle histories.

Specification. For pure strain controlled loading generating the composite cycle requires simply determining the order of the M different load cycles. However, the resulting strain range is independent of this order for strained controlled loading and for each case is simply the greatest algebraic difference between the cycle strain and any other cycle strain.

3.2.3 Comparison between methods

Table 3.1 shows the parameters used to generate 300 random strain histories. The analysis calculated use fractions for each of the EPP+SMT cycle summation options described above along with the distance from the interaction diagram, the creep use fraction, and the fatigue use fraction for ASME Section III, Division 5 design by inelastic analysis.

Of the EPP+SMT options presented in the previous subsection Option A is the closest to an exact method for cycle summation. Of course, as described above it is not a practical method for a realistic structural component requiring a shakedown analysis to establish the design strains. Figure 3.6 compares Options B, C, D, and E to Option A by plotting the number of times the particular alternate predicts a larger, more conservative damage fraction or a smaller, less conservative damage fraction than Option A. The results show that Option B is significantly unconservative, Option C can be unconservative, and Options D and E are both always conservative.

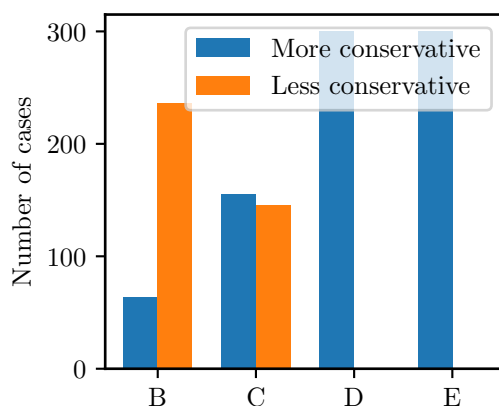


Figure 3.6: Bar chart comparing the number of times the predicted cyclic life fraction from Options B, C, and D exceeds or fails to exceed the life fraction predicted by Option A.

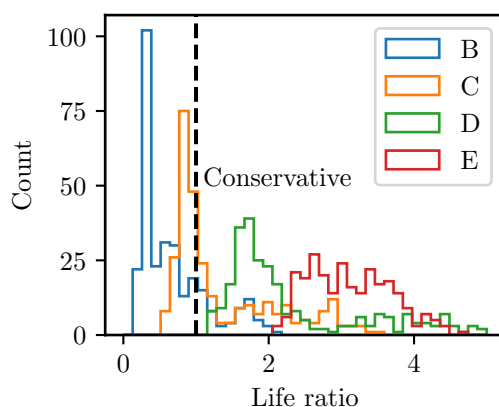


Figure 3.7: Histogram comparing the life ratio between each of Options B, C, and D and Option A. Cases to the right of the dashed line are conservative.

Figure 3.7 shows a different view of this data. This figure plots histograms for Options B, C, D, and E showing the ratio of the use fraction predicted by the relevant option divided by the use fraction for Option A. Values on the histogram greater than 1.0, indicated with a dash line, are conservative. This plot shows that Option B can be significantly unconservative. When it underestimates the usage fraction Option C tends to underestimate the use fraction by less than 50%, which likely falls in the experimental data scatter for actual creep-fatigue tests. When it overestimates the use fraction tends to significantly overestimate it. Option D is moderately conservative compared to Option A and Option E is very conservative. This analysis shows that Option B – individual cycle analyses – is clearly not suitable. Option C – individual cycle analyses superimposed – may be acceptable but is not always conservative. Option D is always conservative but essentially uses a design factor to shift the results of Option C. Option E – the composite cycle approach – is always very conservative.

3.2.4 Comparison to design by inelastic analysis

The different EPP+SMT methods can also be compared to the inelastic analysis results. Figure 3.8a, b, c, d, and e makes this comparison as a function of the creep and fatigue damage calculated for the inelastic method. Each subfigure plots points as (D_f, D_c) ordered pairs on the 316H creep-fatigue interaction diagram. The points inside the design envelope pass the ASME Section III, Division 5 design by inelastic analysis creep-fatigue criteria and the points outside the envelope fail the criteria. The colors of the points indicate whether they pass or fail the consistent EPP+SMT analysis with the cycle combination method given the figure caption.

The figure shows that the consistently-constructed SMT design curves are very conservative – all the random load histories examined here except one fail the SMT design criteria. However, as discussed in a companion report, this is a flaw in this approach towards constructing SMT design charts. The design charts recommended for use with the final EPP+SMT method will be constructed by fitting to creep-fatigue and SMT test data directly, not by attempting to make the method conform to the current ASME design data. However, this comparison was valuable in that it does not reveal any potential nonconservatism with any of the options for load cycle combination.

3.3 Recommended approach: modified composite cycles

Option E – the composite cycle approach – is both conservative and conforms to current ASME practice for design methods using EPP analysis. Therefore, it serves as the basis for the recommended cycle combination approach for the EPP+SMT method. However, there is a complication. The current ASME EPP approaches use the total design life to determine the pseudoyield stress for the analysis. The EPP+SMT approach uses the cycle period. It is not immediately clear how to select the correct cycle period when analyzing a composite load cycle consisting of multiple service loadings. Therefore, we recommend the following modified approach.

1. Begin with a histogram defining each Service Load as transient pressures, mechanical forces, and temperatures or thermal boundary conditions. Figure 3.9a shows an example. The dimensions or units of the loads defined in the table are arbitrary for the sake of this example.
2. Develop one or more composite cycles. These composite cycles are generated by stitching together one or more repetitions of individual Service Loads into a single cycle. Each region of the composite cycle should be clearly identified with a particular Service Load. The composite cycle must be periodic – it must start and end at the same pressures, mechanical loads, temperature and/or thermal boundary conditions. If necessary the designer may postulate a load not defined in the Design Specification in order to appropriately stitch together a set of Service Load conditions (Figure 3.9b). The number of composite cycles and the ordering of each individual service loading within a composite cycle should be guided by any information about the expected ordering of Service Loads in actual operation. For example, the Design Specification may provide information of this kind.

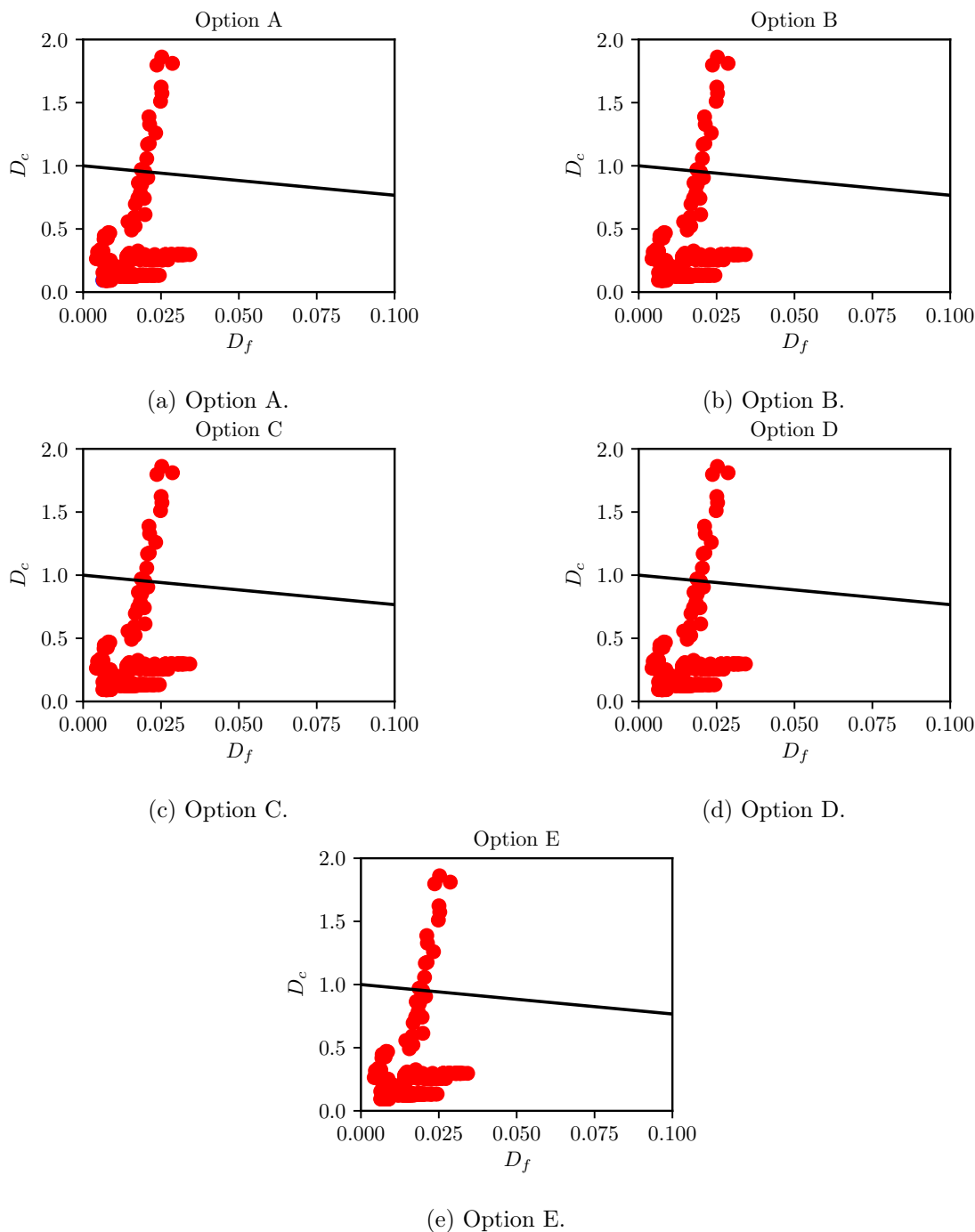


Figure 3.8: Comparison between the ASME Section III, Division 5 design by inelastic analysis method for creep-fatigue evaluation and the EPP+SMT method with consistent design charts. Subfigures a, b, c, d, and e plot data for Options A, B, C, D, and E, respectively. The points are located at the fatigue and creep damage calculated with the design by inelastic analysis method. The black line shows the interaction diagram. The colors indicate the EPP+SMT results: blue means the load combinations pass the EPP+SMT method, red means they fail. Note none of the conditions examined here pass the current EPP+SMT criteria (see text for additional details).

3. Assign a number of cycle repetitions to each individual loading within each composite cycle (Figure 3.9b), hereafter referred to as the loading weight W_i . This information is metadata – it does not imply that the load condition is actually repeated the indicated number of times, either within the composite cycle or in terms of total analysis repetitions of the composite cycle. A load region may be assigned zero weight in a particular composite load cycle. Any new loads defined to meet the cycle periodicity requirements should be assigned zero weight. In assigning these weights the total number of repetitions assigned to a region representing a particular Service Load in all composite cycles must sum to the total repetitions of that Service Load in the Design Specification.
4. Determine the cycle period corresponding to each composite cycle. This cycle period is the total time of the Service Loads assigned to each individual composite cycle, accounting only for the actual repetitions of the loading within the composite cycle and not the product of this time and the weight factors. Fictitious loads used to enforce periodicity shall be assigned zero time in this calculation (Figure 3.9b).
5. For each composite cycle determine the pseudoyield stress using the calculated composite cycle period and the EPP+SMT method. Complete a shakedown analysis of each composite cycle using this pseudoyield stress to generate a periodic history of strains, stresses, and temperatures (Figure 3.9c). The EPP analysis may neglect hold times and use arbitrary loading rates, as the analysis method is rate independent.
6. Within each region of each composite cycle representing a Service Load, use the EPP stress history to find the maximum Huddleston factor. Use this Huddleston factor and Eq. 2.23 to calculate an effective strain range for each region in the composite load cycle. Calculating an effective strain requires two points in time: a reference point and the current time under consideration. When defining the effective strain range for a particular region, the designer should find the maximum effective strain for any reference point in the cycle, but only current times in the region under consideration. Record the effective strain range for each region of each composite cycle. Determine a corresponding Service Load time, which is the total time at the particular Service Load conditions, including time during loading transients. Determine the maximum metal temperature over that region of the composite cycle. Using this strain range, time, and temperature determine an allowable number of design repetitions N_i using the SMT design charts (Figure 3.9c).
7. Calculate the usage fraction of the component at each material point using the equation

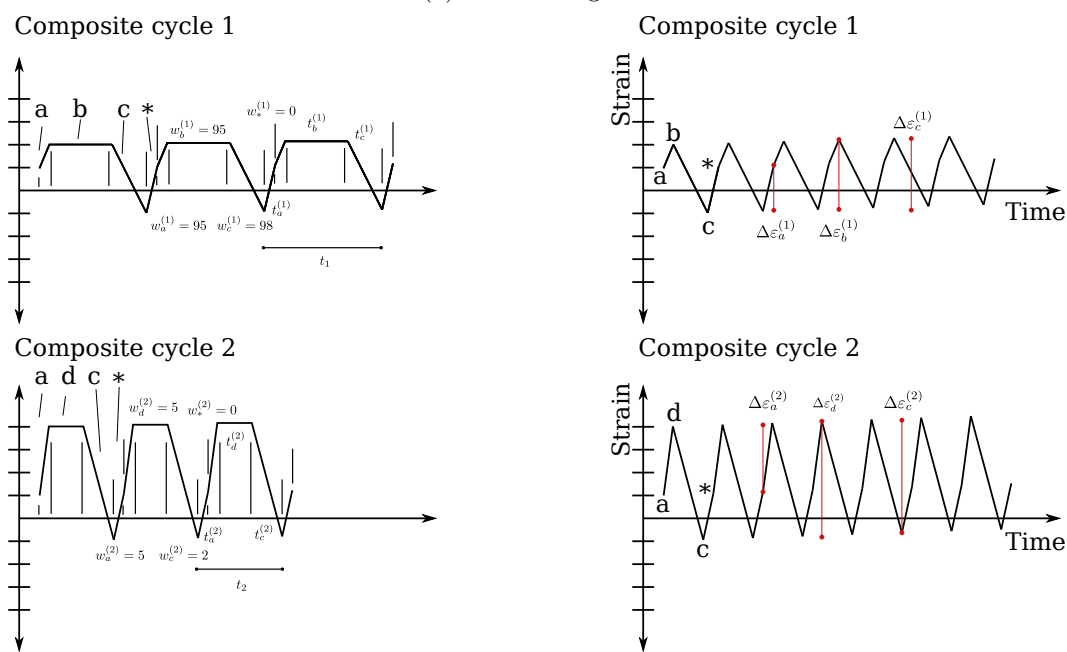
$$D_{SMT} = \sum_{i=1}^{N_{all}} \frac{W_i}{N_i} \quad (3.2)$$

where the sum proceeds over all regions of all composite cycles. If this sum is less than 1.0 for all points in the component then the component passes the EPP+SMT design check.

This proposed approach using the composite cycle, which was demonstrated to be conservative in this report. It lessens the overconservatism of the method by allowing the designer to split the load history into multiple composite cycles. This means that the strain range associated with each Service Load will not necessarily consider the worst possible combination of minimum and maximum loading conditions, but instead something more appropriate for the actual reactor operating conditions, where known. It also allows the use of a reasonable cycle period, rather than the design life, in the EPP calculation. The approach allows the use of a single composite load cycle. In general, using a single composite loading will be very conservative.

Cycle	Repetitions	Load value
a	100	1
b	100	-1
c	100	2
d	5	4

(a) Load histogram.



(b) Composite cycles.

(c) Analysis results.

Figure 3.9: Illustration of the proposed composite cycle approach. (a) Load histogram. (b) Composite cycles developed from the load histogram. Regions assigned to each Service Load, weights, and the composite cycle periods are indicated on the plot. Load conditions marked with a * are fictitious connector segments. (c) Notional analysis results from a shakedown analysis of each composite load cycle. The effective strain range and individual service load time are indicated on the figure.

4 Conclusions

This report describes methods for extending the EPP+SMT creep-fatigue design approach to account for multiaxial loading and for combining different load types. A final recommendation on an effective strain measure must await the development of multiaxial SMT test. In the interim we recommend retaining the current ASME definition of effective strain range. The report explores several alternate load cycle combination techniques before recommending a modified composite cycle methodology.

This report, taken in conjugation with a past report on the strain range estimation procedure [8] and companion reports on developing SMT design curves and on the single-bar SMT method provide a complete creep-fatigue design method. Future work must validate the approach against new SMT test data, component tests, field experience, and by comparison to existing design methods. Preliminary results indicate the new approach is simpler to execute and less over conservative than the current ASME approaches to creep-fatigue design. Once validated, the method can be codified in an ASME nuclear Code Case in order to give designers a simpler, more effective method for the creep-fatigue design of high temperature structural components.

Acknowledgments

The research was sponsored by the U.S. Department of Energy, under Contract No. DE-AC02-06CH11357 with Argonne National Laboratory, managed and operated by UChicago Argonne LLC. Programmatic direction was provided by the Office of Nuclear Reactor Deployment of the Office of Nuclear Energy. The authors gratefully acknowledge the support provided by Sue Lesica, Federal Manager, Advanced Materials, Advanced Reactor Technologies (ART) Program, and Gerhard Strydom of Idaho National Laboratory, National Technical Director, ART Gas-Cooled Reactors Campaign.

Bibliography

- [1] American Society of Mechanical Engineers, “Section III, Division 5,” in *ASME Boiler and Pressure Vessel Code*, 2017.
- [2] R. I. Jetter, “An Alternate Approach to Evaluation of Creep-Fatigue Damage for High Temperature Structural Design Criteria,” in *Fatigue, Fracture and High Temperature Design Methods in Pressure Vessel and Piping*, American Society of Mechanical Engineers Press, 1998.
- [3] Y. Wang, M. C. Messner, and T.-L. Sham, “Report on the FY18 Uniaxial Material Model Testing and Key Feature Test Articles Testing of Grade 91,” tech. rep., Oak Ridge National Laboratory ORNL/TM-2018/885, 2018.
- [4] Y. Wang, R. I. Jetter, M. C. Messner, and T.-L. Sham, “Report on FY18 Testing Results in Support of Integrated EPP-SMT Design Methods Development,” tech. rep., Oak Ridge National Laboratory ORNL/TM-2018/887, 2018.
- [5] Y. Wang, R. I. Jetter, and T.-L. Sham, “Report on FY17 Testing in Support of Integrated EPP-SMT Design Methods Development,” tech. rep., Oak Ridge National Laboratory ORNL/TM-2017/351, 2017.
- [6] Y. Wang, R. I. Jetter, and T.-L. Sham, “FY16 Progress Report on Test Results In Support Of Integrated EPP and SMT Design Methods Development,” tech. rep., 2016.
- [7] Y. Wang, R. I. Jetter, K. Krishnan, and T.-L. Sham, “Progress Report on Creep-Fatigue Design Method Development Based on SMT Approach for Alloy 617,” tech. rep., Oak Ridge National Laboratory ORNL/TM-2013/349, 2013.
- [8] M. C. Messner, T.-L. Sham, Y. Wang, and R. I. Jetter, “Evaluation of methods to determine strain ranges for use in SMT design curves,” tech. rep., Argonne National Laboratory ANL-ART-138, 2018.
- [9] ITER IDoMS, *ITER Structural Design Criteria for In-Vessel Components*. 2012.
- [10] AFCEN, *RCC-MRx*. 2015.
- [11] British Energy, *R5: Assessment Procedure for the High Temperature Response of Structures*. 2001.
- [12] American Society of Mechanical Engineers, “Case N-861: Satisfaction of Strain Limits for Division 5 Class A Components at Elevated Temperature Service Using Elastic-Perfectly Plastic Analysis,” in *ASME Boiler and Pressure Vessel Code, Nuclear Component Code Cases*, 2015.
- [13] American Society of Mechanical Engineers, “Case N-862: Calculation of Creep-Fatigue for Division 5 Class A Components at Elevated Temperature Service Using Elastic-Perfectly Plastic Analysis,” in *ASME Boiler and Pressure Vessel Code, Nuclear Component Code Cases*, 2015.

- [14] D. R. Hayhurst and J. T. Henderson, "Creep stress redistribution in notched bars," *International Journal of Mechanical Sciences*, vol. 19, no. 3, pp. 133–146, 1977.
- [15] H. T. Yao, F. Z. Xuan, Z. Wang, and S. T. Tu, "A review of creep analysis and design under multi-axial stress states," *Nuclear Engineering and Design*, vol. 237, no. 18, pp. 1969–1986, 2007.
- [16] D. R. Hayhurst, "Creep of metals under multi-axial states of stress," *Journal of the Mechanics and Physics of Solids*, vol. 20, pp. 381–390, 1972.
- [17] E. J. Chubb and C. J. Bolton, "Stress state dependence of creep deformation and fracture in AISI type 316 stainless steel," in *International conference on engineering aspects of creep*, (London), pp. 39–48, 1980.
- [18] R. L. Huddleston, "An Improved Multiaxial Creep-Rupture Strength Criterion," *Journal of Pressure Vessel Technology*, vol. 107, no. November, pp. 421–429, 1985.
- [19] J. Henderson and J. D. Snedden, "Prediction of shear-creep failure in aluminum-alloy components," *Journal of the Institute of Metals*, vol. 100, pp. 163–171, 1972.
- [20] J. Henderson and J. D. Snedden, "Creep fracture of copper cylindrical bars under pure torque," in *Creep in structures* (J. Hult, ed.), (Gothenburg), Springer-Verlag, 1972.
- [21] D. R. Hayhurst, "A biaxial-tension creep-rupture testing machine," *The Journal of Strain Analysis for Engineering Design*, vol. 8, no. 2, 1973.
- [22] F. A. Leckie and C. J. Morrison, "Creep rupture of notched bars," *Proceedings of the Royal Society of London. Series A, Mathematical and Physical Sciences*, vol. 360, no. 1701, pp. 243–264, 1978.
- [23] V. Tvergaard, "Analysis of creep rupture in a notched tensile bar," *Mechanics of Materials*, vol. 4, no. 2, pp. 181–196, 1985.
- [24] G. A. Webster, S. R. Holdsworth, M. S. Loveday, K. M. Nikbin, I. J. Perrin, H. Purper, R. P. Skelton, and M. W. Spindler, "A Code of Practice for conducting notched bar creep tests," *Fatigue and Fracture of Engineering Materials and Structures*, vol. 27, pp. 319–342, 2004.
- [25] J. Lubliner, *Plasticity Theory*. Mineola, New York: Dover Publications, 2008.
- [26] R. L. Huddleston, "Two-Parameter Failure Model Improves Time- Independent and Time- Dependent Failure Predictions," tech. rep., Lawrence Livermore National Laboratory, 2003.
- [27] V.-T. Phan, M. C. Messner, and T.-L. Sham, "A Unified Engineering Inelastic Model for 316H Stainless Steel," in *Proceedings of the 2019 ASME Pressure Vessels and Piping Conference*, 2019.



Applied Materials Division

Argonne National Laboratory
9700 South Cass Avenue, Bldg. 212
Argonne, IL 60439

www.anl.gov



**U.S. DEPARTMENT OF
ENERGY**

Argonne National Laboratory is a U.S. Department of Energy
laboratory managed by UChicago Argonne, LLC